The International Journal of Advanced Manufacturing Technology (2021) 114:1803–1817
https://doi.org/10.1007/s00170-021-06947-1

ORIGINAL ARTICLE

A comparative study on the surface integrity of single-step and multi-step sequential machining in electric discharge machining

Guisen Wang [1,2] · Fuzhu Han [1,2]

Received: 15 June 2020 / Accepted: 16 March 2021 / Published online: 3 April 2021

Abstract

In the past, the effect of electrical parameters, dielectric, and electrode material and shape on surface integrity in electric discharge machining (EDM) was widely studied by scholars. However, these researches are mainly based on single-step EDM that can be categorized into either roughing or finishing. The production of components by EDM is a process from roughing to finishing in industry, which is a multi-step machining process. Therefore, in order to provide a better guideline for the fabrication of parts through the single-step EDM approach (refers to the last step of multi-step machining in this study), it is necessary to investigate and quantify the difference in surface integrity between single-step and multi-step sequential machining. In this study, the surface integrity of single-step and multi-step machined samples is evaluated and compared. The results demonstrate that the surface roughness, white layer thickness, and surface residual stress of multi-step machined samples are higher than those of single-step machined samples. In the finishing stage, the difference in surface roughness and residual stress between them becomes even larger. It was indicated that the surface state of the sample obtained in the previous processing steps has an influence on the final machining quality during multi-step sequential EDM. In addition, the change of the surface morphology of the tool electrode caused by the previous machining steps would also affect the surface roughness of the workpiece processed in the current step. There is no significant difference in the crystalline phase between single-step and multi-step sequential machining.

Keywords Electric discharge machining · Morphology · Surface roughness · White layer · Residual stress

1 Introduction

Electric discharge machining (EDM) is a very important non-traditional machining process, which has been routinely utilized to manufacture components and parts in the areas of aviation, aerospace, and automotive industry [1]. The increasing use of EDM in the manufacturing industry mainly attributes to the following two factors. On the one hand, it can be used to fabricate all kinds of electro-conductive materials without considering their physical and metallurgical properties [2]. In particular, it is suitable for machining difficult-to-machine materials such as superalloys and cemented carbides. On the other hand, it can be applied to producing geometrically complex shapes and a low stiffness workpiece [3, 4]. During the process of EDM, tool and workpiece electrodes are immersed in the dielectric fluid and separated by a small gap. When a voltage pulse is applied across the electrodes, and the gap distance is small enough, a spark discharge will occur within the inter-electrode gap [5]. The amount of heat generated by spark discharge can raise electrode temperatures locally up to tens of thousands of degrees Celsius in pulse discharge duration [6]. Such a high temperature is enough to melt, vaporize, and even ionized all materials. Accordingly, materials are ejected from the workpiece and flushed away by the dielectric fluid. In the process of repeated discharge, the material is continuously removed and the objective shape is finally obtained.

There is a certain thickness of the metamorphic layer on the component and part surface after EDM. The generation of a metamorphic layer on the machined surface attributes to thermal energy caused by sparks during EDM. Some defects, such as voids, cracks, and debris, can be found on the surface of the metamorphic layer, which would lead to a complete aggravation of the mechanical properties of components. Therefore, it

✉ Fuzhu Han
hanfuzhu@mail.tsinghua.edu.cn

[1] Department of Mechanical Engineering, Tsinghua University, Beijing 100084, China

[2] Beijing Key Lab of Precision/Ultra-precision Manufacturing Equipment and Control, Tsinghua University, Beijing 100084, China

is essential to evaluate the surface integrity of samples after EDM. Surface integrity is a technical index to describe, identify and control various changes that may occur on the surface and sub-surface of the part during the machining process, which has an important influence on the functional performance. When the surface integrity of the electric discharge machined (EDMed) component is poor, the failure is easy to occur during the application process [7]. Surface integrity in EDM is usually characterized by surface roughness, the thickness of the white layer, and residual stress, etc. [7, 8]. In recent years, it has attracted extensive attention of a variety of researchers all over the world.

Surface integrity issues stem from inhomogeneous material alteration, which is led by mechanical loading, thermal gradients, and phase transformations during processing [9, 10]. It is complicated and affected by workpiece/electrode material, electricity parameter, and dielectric in EDM, as summarized in Fig. 1. For a certain workpiece and electrode material, surface integrity in EDM is affected primarily by electricity parameter and dielectric. It is reported that electricity parameters such as discharge current (I_p) and pulse-on time (t_{on}) played an important role in influencing surface integrity [11–13]. In general, the surface roughness of the workpiece increases with the increase of I_p and t_{on} [14, 15]. Hence, lower I_p and t_{on} produced a better surface finish. However, Lee [8] and Rizvi [16] found that increasing t_{on} does not necessarily increase the surface roughness of the workpiece while the other parameters remain the same. The decrease of the surface roughness can be associated with the very long discharge duration that leads to excessive diameter growth of the plasma channel, and thus the pressure of the plasma over the molten cavities declined. Consequently, the ejection of material from the molten cavities of the workpiece and tool electrode at the end of pulse duration happened insufficiently. This phenomenon probably generates a lower surface roughness on the workpiece [17]. In addition to the electricity parameters, dielectric fluid is also an essential factor affecting surface roughness. The surface roughness of the workpiece produced by EDM in deionized water is commonly lower than that in hydrocarbon oils [18]. Kumar et al. found that the EDM oil with alumina micropowder was conducive to decrease surface roughness because it could increase the wider gap between electrodes, further to obtain a better flushing condition [19].

It is reported that only about 15% of the molten material can be removed from the workpiece during EDM [20]. The remaining molten materials are rapidly cooled and eventually formed a recast layer on the workpiece surface. This layer is very difficult to etch, and it is apparently white under an optical microscope. Thus, it is also known as the white layer. The examination of the white layer indicated that it is heavily alloyed with the pyrolysis products from the dielectric and the tool electrode [8, 21]. Previous studies suggested that I_p and t_{on} are direct ratios with the thickness of the white layer [8, 15]. Because the higher I_p or t_{on} causes more discharge energy at the sparking zone. The discharge energy can be converted into heat to melt more materials. Bozkurt et al. showed that the quantity of molten metal on the surface of the workpiece washed away by the dielectric is constant during EDM [22]. High I_p and t_{on} bring more discharge energy, and it can increase the amount of molten material that is not completely removed from the workpiece by flushing. Therefore, white layer thickness increases with the increase of I_p and t_{on}. Dielectric also plays an important role in improving white layer thickness. Pecas and Henriques reported that powder-mixed dielectric was beneficial to the reduction of white layer thickness [23]. The effect of the type and size of powder on white layer thickness was investigated by Tzeng and Chen [24]. They found that particle size has an opposite influence

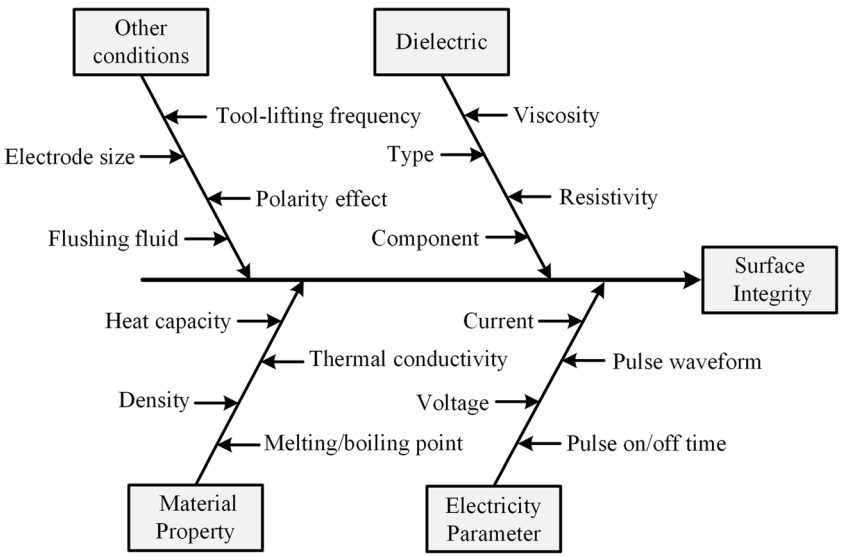

Fig. 1 Fishbone chart analysis for surface integrity of the EDMed sample

on the thickness of the recast layer, and Al powder generated the thinnest white layer in the EDM of SKD-11 among Al, Cr, SiC, and Cu powders.

The generation of residual stresses on the EDMed samples is mainly due to the nonuniformity of heat flux and metallurgical transformations or local inhomogeneous plastic deformation [25]. Generally, the residual stress on the surface of EDMed samples is shown as tensile stress, which increases with the increase of pulse energy. Tang and Yang simulated thermal phase transformation and residual stress in a single pulse EDM process by the numerical simulation method [25]. Compared with the t_{on}, the I_p has a more significant influence on maximal tensile stress. However, the effect of t_{on} on the depth location of the maximal tensile stress is more important than that of I_p. Liu and Guo proposed a novel model to simulate residual stress in the case of massive random discharges during EDM [26]. The results indicated that the maximum value of the average residual stress slightly increased with the increase of the discharge voltage (U_p). However, the surface average residual stress decreased when increasing voltage. In addition, many researchers have studied the influence of processing conditions on residual stress by experimental [2, 27–29]. It was found that I_p would affect the surface residual stress, and t_{on} would influence the depth of distribution of the stress. Moreover, pulse interval (t_{off}) also impacts the stress distribution, and the occurrence of the stress range increases with the decrease of the t_{off}. Li et al. investigated the effect of processing liquid on residual stress in EDM [29]. They found that the residual stress of the EDMed sample in water was higher than that in kerosene owing to cooling capacity and surface physical properties. Generally, surface residual stress would not be greater than the tensile strength of materials.

Although the influence of EDM conditions (e.g., electrical parameters and dielectric) on surface integrity has been widely studied, the surface integrity evolution and the effect of the previous processing steps on final processing quality in multi-step sequential EDM is seldomly reported. Multi-step processing is composed of several independent single steps, wherein different processing parameters are involved. Single-step machining is to process with a single processing parameter in only one step, specifically, the last step in multi-step processing. In fact, the fabrication of components by EDM is a process from roughing to finishing in industry (multi-step sequential EDM). It is unreasonable to apply the theory which originated from single-step processing to guide actual production. This is because the surface states of the sample produced by the previous machining operations may have an impact on the current processing. Up to now, the difference of surface integrity between single-step and multi-step sequential EDM is still not very clear, seldomly reported before. Therefore, this study aims to investigate the difference in surface topography, roughness, crystalline phase, white layer thickness, and residual stress between single-step and multi-step sequential EDM. Meanwhile, the evolution of surface integrity during multi-step sequential EDM was also researched. The present study points out some necessary issues to be noted when using single-step processing to guide actual production in EDM.

2 Materials and methods

2.1 Materials

STAVAX steel was selected as a work material in this study, which was commonly used in the mold industry owing to its outstanding mechanical properties and terrific corrosion resistance. The composition of STAVAX steel was shown in Table 1. The dimension of the workpiece was 60 × 60 × 4 mm^3. They were stress relieved before EDM for ensuring stress-free conditions. Oxygen-free copper (TU1) was selected as an electrode material (Table 2). The diameter and length of the electrode material were 15 mm and 110 mm, respectively.

2.2 Machining experiments setup

The experiment was performed by an industrial EDM (EDGE3S, MAKINO, Japan). Commercial grade EDM oil served as the dielectric. The selection of EDM parameters is based on the recommended values in the manual. Table 3 presented the EDM parameter settings adopted in this study. Tables 4 and 5 showed the processing of different samples by EDM. In this study, we found through experiments that the effect of machining depth on surface integrity can be ignored for single-step machining. For example, the Ra value of S-3 with the EDM depth of 0.2 mm and 1.2 mm was 1.39 μm and 1.405 μm, respectively. No significant difference between them was observed. Therefore, to save processing time, the EDM depths of samples were set to 0.2 mm and 1.2 mm for single-step and multi-step machining, respectively. Table 6 presented the processing depth of each step in the multi-step machining. In this table, the processing depths of each process step have been given except for process No.1. The processing depths of process No.1 was determined by the total processing depth and the number of processing steps. For example, for sample M-1 and M-2, the processing depth of process No.1 was 0.51 mm and 0.45 mm, respectively. The schematic diagram of single-step and multi-step machining was displayed in Fig. 2. The EDM machine tool and tool electrode were shown in Fig. 3.

Table 1 Composition of workpiece material (weight percent)

C	Si	Mn	Cr	V	Fe
0.38	0.9	0.5	13.6	0.3	Balance

Table 2 Composition of electrode material (weight percent)

Cu+Ag	P	Bi	Sb	As	Fe	Ni	Pb	Sn	S	Zn	O
99.97	0.002	0.001	0.002	0.002	0.004	0.002	0.003	0.002	0.004	0.003	0.002

2.3 Investigation of surface topography and crystalline phase

Surface topography of different EDMed samples was characterized by a field emission scanning electron microscope (SEM). Three-dimensional topographies were measured using a laser scanning microscope (LSM). The crystalline phase was determined by X-ray diffraction (XRD). The scan was performed in the range of 20–90° with an angle of the incident beam of 0.02°.

2.4 Testing surface roughness

The EDM surface is composed of many non-directional craters and hard convex edges. Hence, it only needs to investigate the surface roughness of the sample produced by EDM in one direction. In this study, we used arithmetic mean height (Ra) and the maximum height of the profile (Rz) to characterize the surface roughness of samples. Ra and Rz were calculated by Eqs. (1) and (2), respectively. l_r means the measured length, x is the boundaries of the measured length, $z(x)$ is the surface height. Surface roughness is determined by a surface roughness profiler (JB-4C) that was shown in Fig. 4.

$$\mathrm{Ra} = \frac{1}{l_r}\int_0^{l_r} |z(x)|dx \tag{1}$$

$$\mathrm{Rz} = \max[z(x)] + \min[z(x)] \tag{2}$$

2.5 White layer thickness measurement

A small piece was cut from the machined sample and embedded in a polymeric resin to investigate its white layer thickness. The section of the sample was polished with abrasive paper. Then, it was ultrasonically cleaned in acetone and anhydrous ethanol, respectively. After that, the polished samples were etched with a Nital (4%) solution. Optical microscopy (DSX 510, Fig. 5a) was used to observe the white layer and measure its average thickness. Figure 5b showed an example of the cross-section and the calculation of the average thickness of the white layer.

2.6 Surface residual stress evaluation

X-ray diffraction is widely used to test the residual stress of components and parts. In this study, surface residual stress was measured by the cosα method using a portable X-ray stress analyzer (μ-X360n, Fig. 6a) [30, 31]. In spite of the minor difference between the cosα method and the sin2ψ method in the accuracy of stress measurement for many metals, the cosα method can be more simple and quick to investigate the residual stress compared with the well-known $\sin^2\psi$ method [30]. Therefore, it is gradually applied in various engineering fields. Figure 6b showed an experimental setup for recording a D-S ring when the X-ray beam is incident on the specimen surface at the tilt angle ψ_0 and the rotation angle ϕ_0. According to the previous study, the residual stress σ_x in the direction of the x-axis can be calculated by Eqs. (3) and (4) [31].

$$\overline{\varepsilon_\alpha} = \frac{1}{2}\left[(\varepsilon_\alpha - \varepsilon_{\pi+\alpha}) + (\varepsilon_{-\alpha} - \varepsilon_{\pi-\alpha})\right] \tag{3}$$

$$\sigma_x = -\frac{E}{1+\vartheta}\frac{1}{\sin 2\eta}\frac{1}{\sin 2\psi_0}\left(\frac{\partial \overline{\varepsilon_\alpha}}{\partial \cos\alpha}\right) \tag{4}$$

The description of some parameters in the foregoing equation is shown in Fig. 6b. In addition to the parameters showed in these figures, ϑ refers to Poisson's ratio, and E is Young's modulus. It is reported that the out-of-plane normal stress (σ_z)

Table 3 Machining conditions

Process no.	1	2	3	4	5	6	7	8	9	10	11
Pulse voltage (V)	190	190	190	190	190	190	190	190	190	143	128
Pulse current (A)	15.8	12.8	9.8	8.7	5.5	5	4	3.1	2.3	1.35	0.9
Pulse-on time (μs)	121	100	74	53	23	11	7	4	2.5	1.2	1.2
Pulse-off time (μs)	30	26	18	28	13	8	7	5.5	5.5	9	9
Electrode polarity	+	+	+	+	+	+	+	+	+	−	−

Table 4 Processing of different samples in single-step machining

Sample number	S-1	S-2	S-3	S-4	S-5	S-6	S-7
Single-step machining	No.5	No.6	No.7	No.8	No.9	No.10	No.11
Processing depth (mm)	0.2	0.2	0.2	0.2	0.2	0.2	0.2

Table 5 Processing of different samples in multi-step machining

Sample number	M-1	M-2	M-3	M-4	M-5	M-6	M-7
Multi-step machining	No.1-5	No.1-6	No.1-7	No.1-8	No.1-9	No.1-10	No.1-11
Processing depth (mm)	1.2	1.2	1.2	1.2	1.2	1.2	1.2

Table 6 Processing depth of each step in multi-step machining

Process no.	1	2	3	4	5	6	7	8	9	10	11
Depth (μm)	Balance	250	200	150	90	60	50	40	30	20	10

can be ignored compared to the in-plane stress, and the average normal stress is isotropic in the surface and subsurface [26]. Therefore, the residual stress of the samples can be expressed by σ_x.

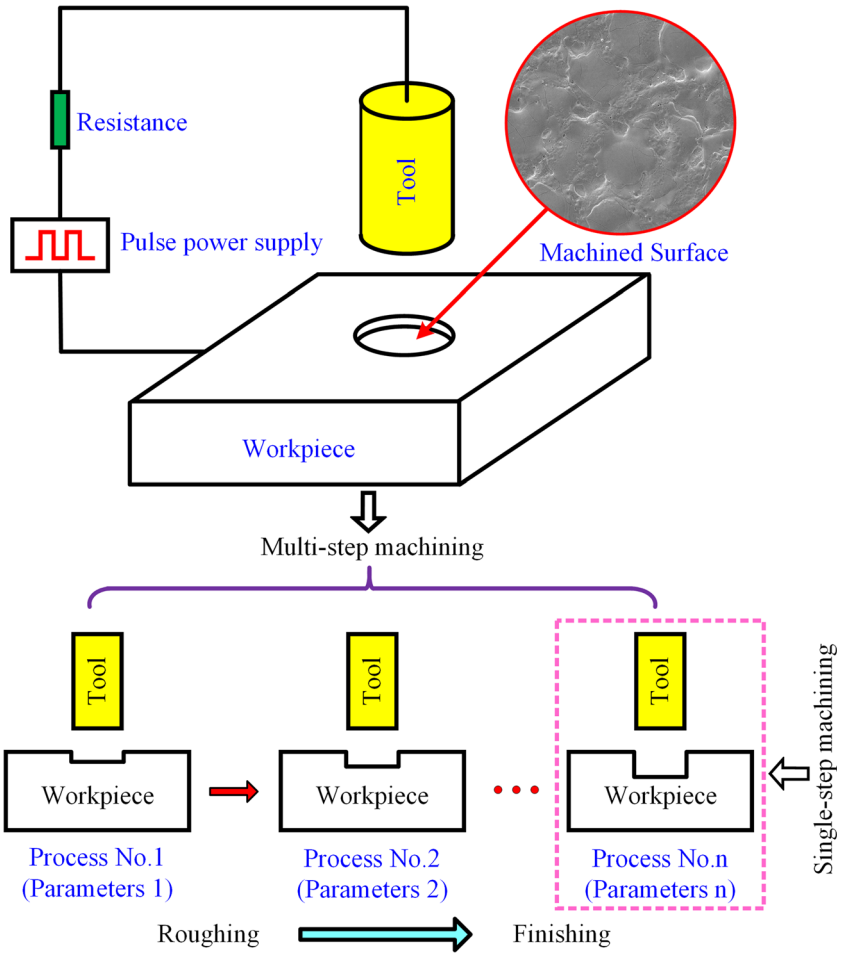

Fig. 2 Schematic diagram of single-step and multi-step machining

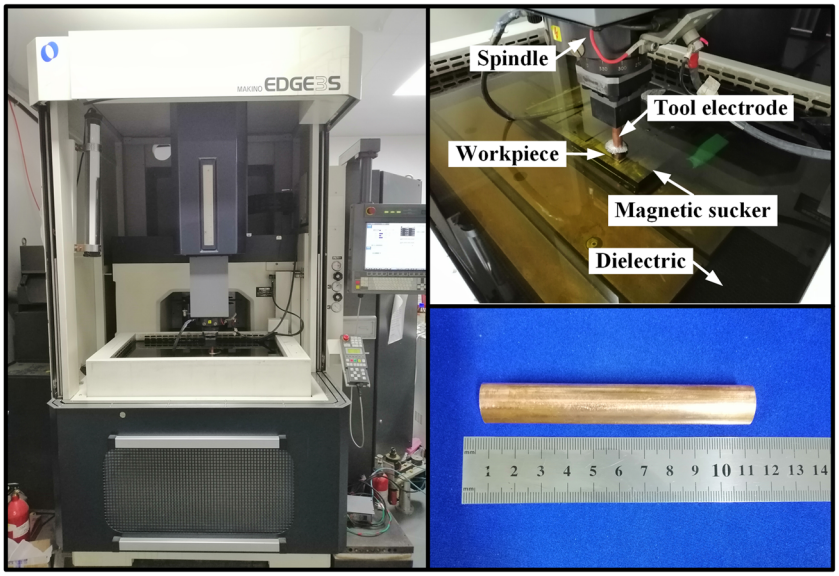

Fig. 3 Machine tool and tool electrode used in EDM experiments

3 Results and discussion

3.1 Surface topography

The morphology of the EDMed surface and its evolution characteristics in multi-step sequential machining were observed with the aid of SEM. As shown in Fig. 7, the sample surface presented lots of non-directional craters and convex edges, which was consistent with the previous studies [6, 16]. Some defects (Fig. 8), such as cracks, debris, and voids, were displayed on the surface of the sample because of rapid heating and cooling during EDM [21]. The formation of cracks on the EDMed surface attributes that the contraction stresses exceeds the ultimate tensile strength of materials in the metamorphic layer [32]. During the process from roughing to finishing in multi-step EDM, the dimension of the craters on the sample surface gradually decreased, and the defects become fewer and fewer. This was mainly attributed to the influence of discharge energy and processing polarity. For sample M-1 to M-5, the changes in surface topography were mainly caused by the gradual decrease of discharge energy per pulse in the process. Jahan et al. found that lower discharge energy would lead to smaller craters [33]. Current and pulse-on time are important factors to determine discharge energy.

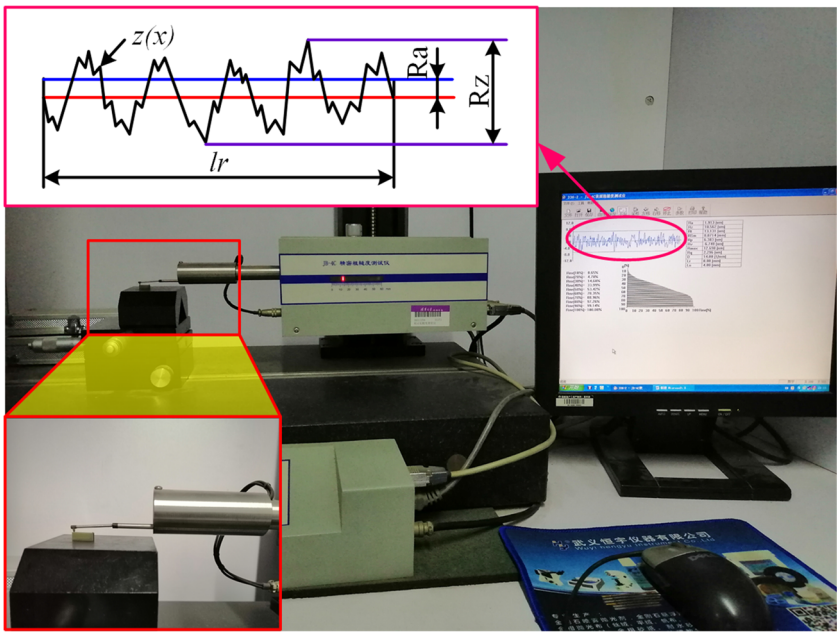

Fig. 4 Surface roughness measurement of samples

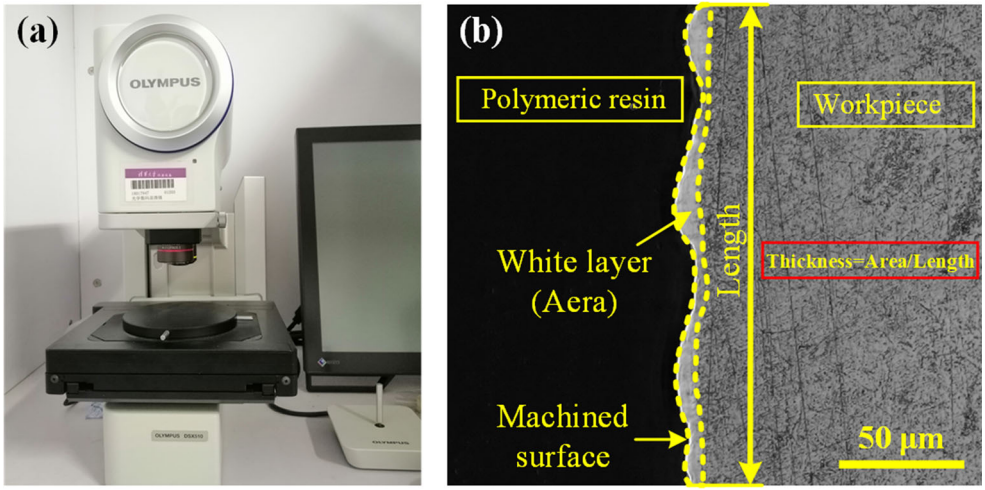

Fig. 5 **a** Optical microscopy, and **b** the calculation of the average thickness of the white layer

The discharge energy decreases with the decrease of pulse-on time and current. Thus, a better surface finish was eventually obtained by the reduction of pulse-on time and current. The difference in surface topography between M-5 and M-6 ascribes to the effect of discharge energy and polarity effect. Compared to M-6, M-7 showed a better surface due to the decrease of pulse current.

To observe the difference between multi-step sequential processing and single-step processing, we also obtained the SEM images of single-step processing. The results were presented in Figs. 9 and 10. It was clear that the surface morphology evolution of the single-step EDMed sample was similar to that of the multi-step EDMed sample. However, the size of the craters on the single-step EDMed surface was smaller than that of the multi-step EDMed surface. Figure 11 displayed the 3D surface topography under different machining conditions, where we could get the same conclusions as before. In conclusion, these results all demonstrated that the previous

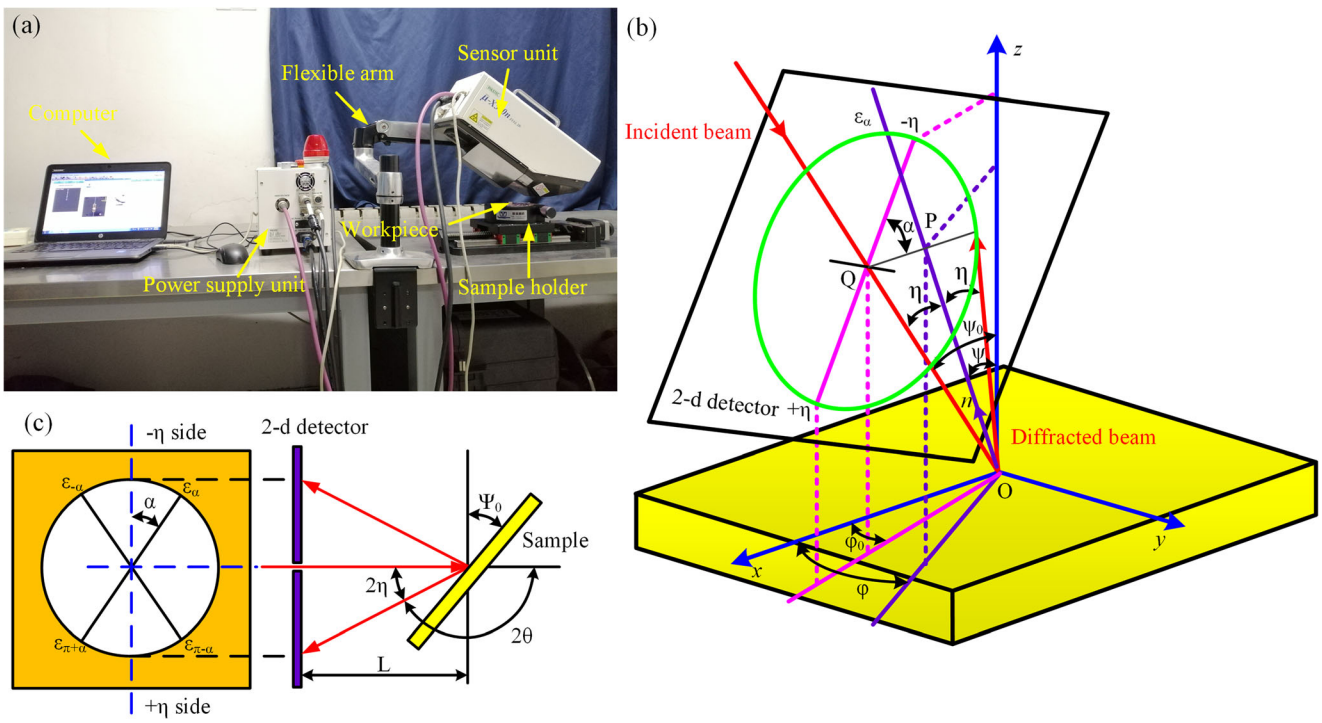

Fig. 6 **a** X-ray residual stress analyzer (μ-X360n), **b** Debye-Scherrer ring recorded on a two-dimensional detector by a single-exposure of X-rays, **c** schematic representation of the four types of strains used for stress calculation based on cosα method

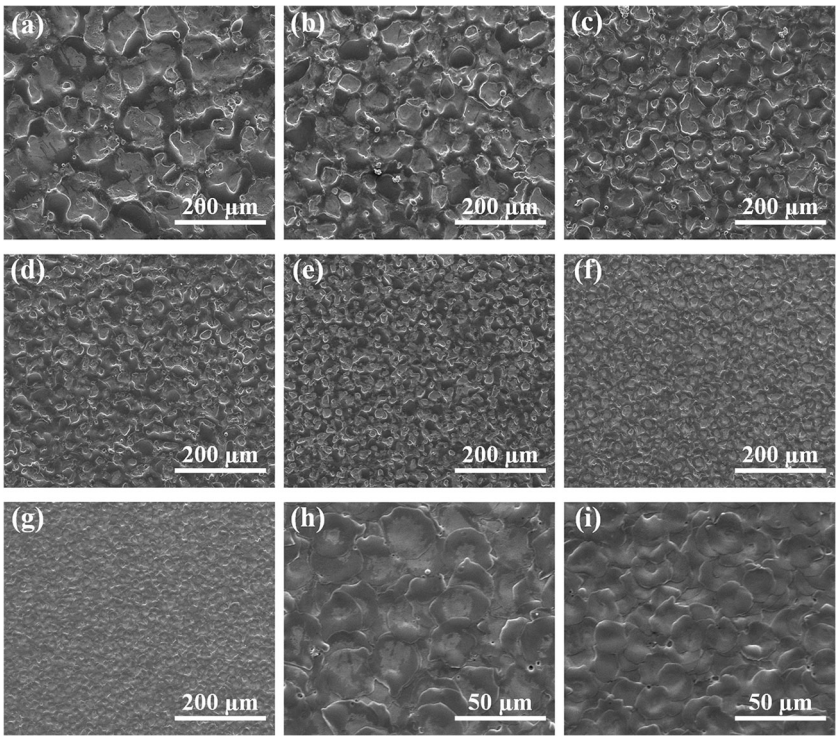

Fig. 7 SEM images of different samples in multi-step machining: **a** M-1, **b** M-2, **c** M-3, **d** M-4, **e** M-5, **f**, **h** M-6, **g**, **i** M-7

step machining will indeed influence the current step machining in the practical application of EDM.

3.2 Surface roughness

The roughness of the EDMed sample surface was investigated by a surface roughness profiler, and the results were presented in Fig. 12. From this figure, it can be seen that the surface roughness (Ra and Rz) from sample M-1 to sample M-7 is gradually reducing. With the decrease of pulse-on time and current, the discharge energy of each pulse decreases. Generally speaking, material removal under low discharge energy is lower than that under high discharge energy. Therefore, the surface processed under low discharge energy conditions was smoother. This means that the surface roughness of EDMed sample was also low at low discharge energy. In addition to discharge energy, polarity also has an important influence on surface roughness. The negative polarity of the workpiece, in general, has an inferior surface roughness than that under positive polarity in EDM [34]. The evolution of the surface roughness of the single-step machined sample is similar to that of the multi-step sequential machined sample. However, the surface roughness of S-X (X = 1-7) was lower than that of M-X. More importantly, the Ra (Rz) value of M-7 is 1.733 (1.526) times that of S-7. In the industry, the products are usually obtained through multi-step processing in EDM. In this regard, it is unreasonable to use the surface roughness obtained by single-step processing to serve as the guideline for multi-step machining especially in the stage of precise machining. This was indicated that the craters on the surface produced in the current step would have an influence on the generation and distribution of the craters in the next step. Moreover, as the electrode could not be replaced during the process of multi-step machining, the structural change of the electrode surface may be another factor to affect the surface roughness.

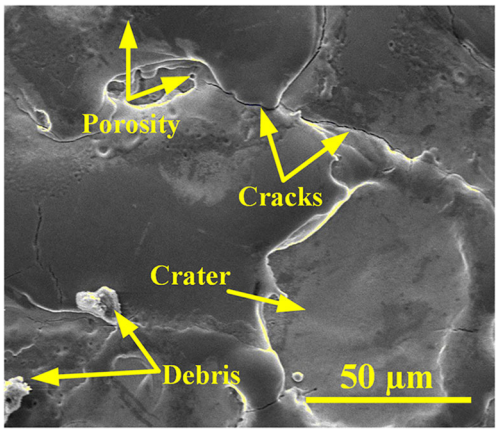

Fig. 8 Micro-cracks on the surface of sample M-1

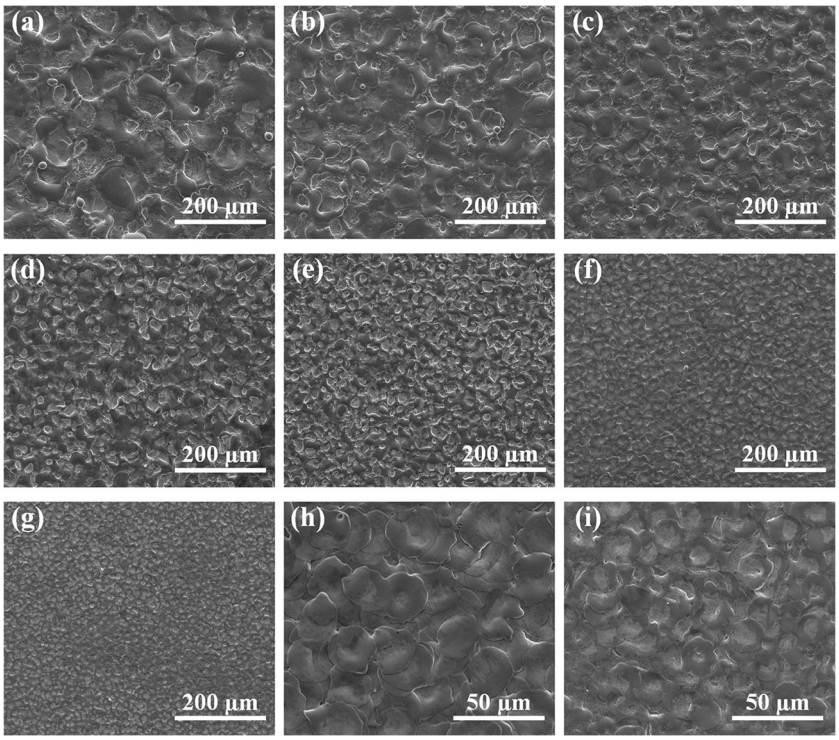

Fig. 9 SEM images of different samples in single-step machining: **a** S-1, **b** S-2, **c** S-3, **d** S-4, **e** S-5, **f**, **h** S-6, **g**, **i** S-7

In order to make clear the difference of surface roughness between multi-step machining and single-step machining, we prepared five groups of samples based on the different manufacturing processes as shown in Fig. 13. For samples B and C, the processing depths of process No. 1 and 7 were 0.25 mm and 0.2 mm, respectively. The processing depth of the other process steps was in accordance with the data given in Table 6. The roughness measurement results were displayed in Fig. 14. Clearly, the surface roughness of B was slightly lower than that of A (0.05 mm in machining depth of the last step). It was indicated that the material removal amount in the last step influences the surface roughness of the sample. Compared with B, the surface roughness of C decreased owing to the replacement of the tool electrode in the last step during EDM. It was illustrated that the surface morphology of the tool electrode also influenced the subsequent processing. From Fig. 7, we could find that the sample surface had lots of non-directional craters and convex edges. Because the surface of the new electrode is very flat, the discharge and material removal would first be carried out on the convex position of the sample surface. The height of the raised part was reduced. Accordingly, the surface roughness of C was lower than that of B. Moreover, the surface roughness of D was lower than that of C. It was demonstrated that the surface topography of the sample produced by previous processing has an impact on the subsequent processing. The difference in the effect of electrode and workpiece morphology on surface roughness may be attributed to the difference in the materials removal amount of cathode and anode. Compared with D, the surface roughness of E slightly decreased, which could be attributed to machining depth. As machining depth increases, debris removal becomes more difficult. This would deteriorate the machining condition, and thus surface quality of the sample becomes worse. As a result, the roughness of the

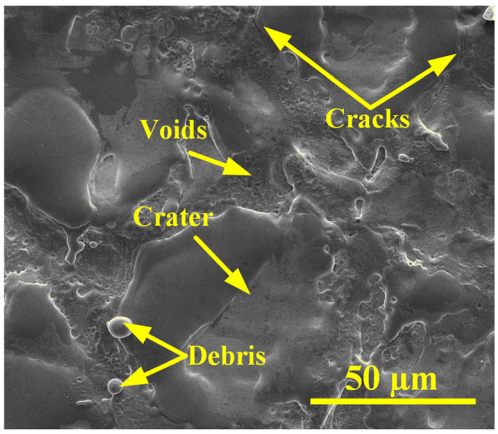

Fig. 10 Micro-cracks on the surface of sample S-1

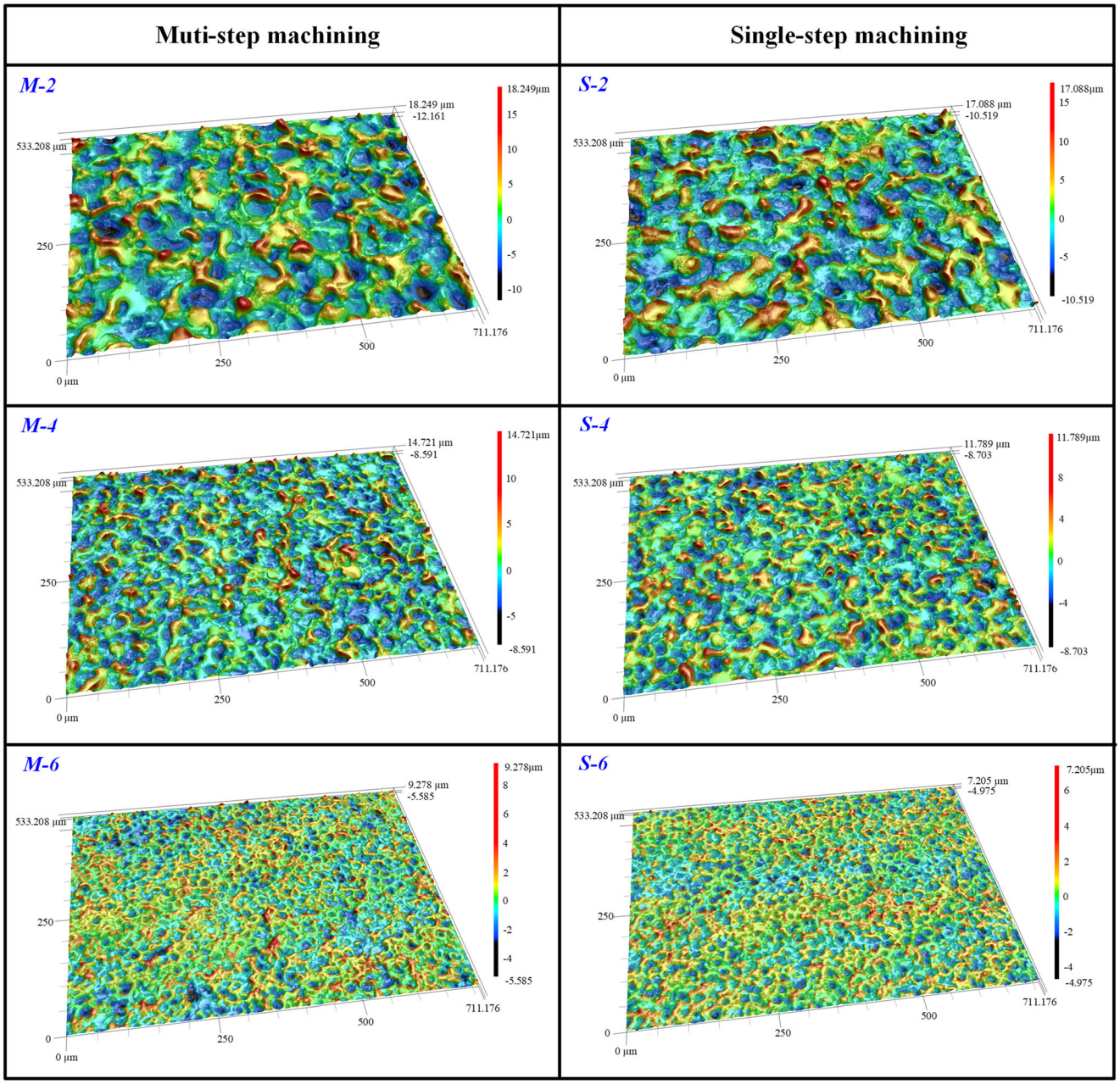

Fig. 11 LSM images of the sample under different machining conditions

multi-step EDMed sample was larger than that of the single-step EDMed sample.

3.3 Phase analysis of EDMed surface

The crystalline phases of the EDMed surface, as measured by XRD, were shown in Fig. 15. In addition to the spectra of the substrate (α-Fe), the peaks of γ-Fe and iron carbides can be seen from the EDMed surface. The results were consistent with previous studies [6, 32]. In EDM, kerosene is cracked to produce carbon, whereby carbon will fuse with the molten metal material. During the cooling process, a series of phase transitions occur in the metal. Therefore, γ-Fe and iron carbides were formed on the surface of EDMed sample. No remarkable difference between multi-step EDMed sample and single-step EDMed sample in crystalline phases was observed. The peak intensity of α-Fe was found to be increased from sample Y-2 (Y=S or M) to Y-6. In addition, a new and weak iron carbide peak could be observed from the surface of M-4, M-6, S-4, and S-6. The small difference in the crystal phase may be related to the difference of discharge energy.

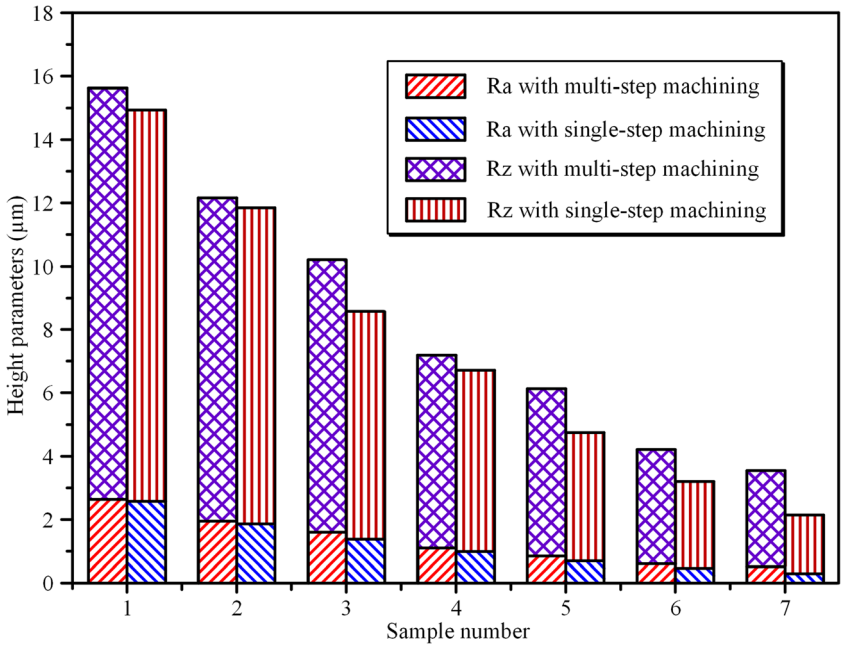

Fig. 12 Surface roughness of single-step and multi-step machined samples

3.4 White layer

It is well known that the surface of the sample will produce a metamorphic layer during EDM (Fig. 16). This layer is composed of the white layer and the heat-affected zone. The formation of the white layer attributes to the molten metal, which has not been removed yet and re-solidified on the sample surface. The heat-affected zone is directly below the white

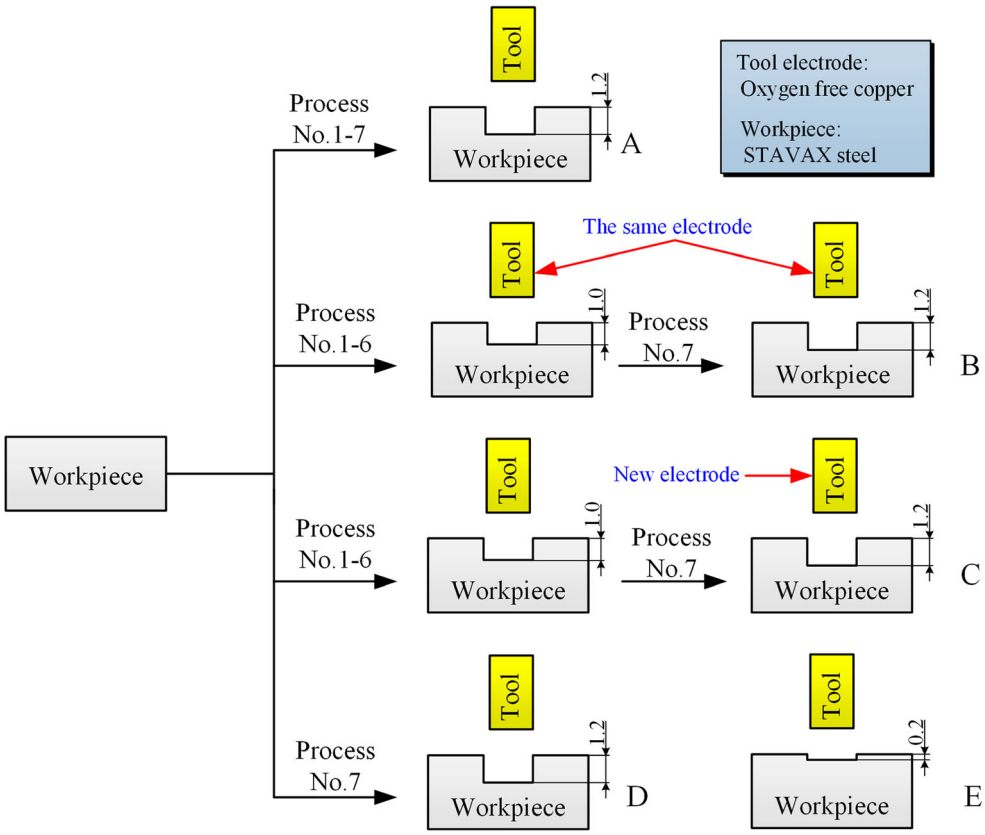

Fig. 13 Manufacturing processes of samples **A**, **B**, **C**, **D**, and **E**

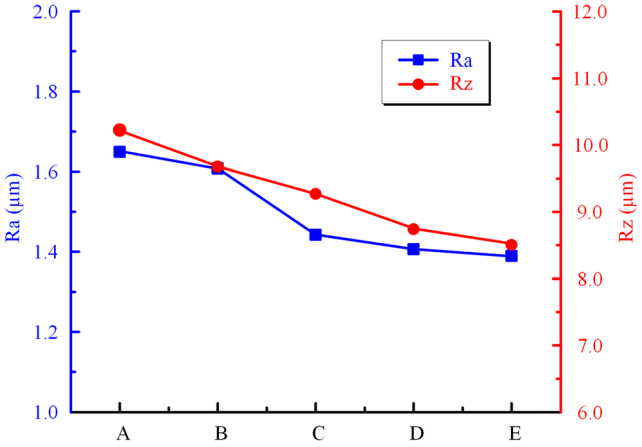

Fig. 14 The surface roughness of EDMed samples under different conditions

layer. Although the material in this area did not melt, its structure got changed due to the effect of heat. The heat-affected zone is made up of several layers, which are hard to discriminate [9]. This zone usually involves residual stresses, phase transformation structures, and micro-cracks, etc. In this study, for the surface metamorphic layer, we focus on researching the evolution of white layer thickness under different machining conditions.

Different regions of each sample were selected, and the average was calculated to investigate the white layer thicknesses, as shown in Fig. 17. Obviously, the thickness of the white layer gradually decreased for single-step EDM. In general, as low pulse energy could lead to the reduction of material melting amount, the white layer thickness decreases when diminishing in pulse energy [32]. Bozkurt et al. found that the amount of molten material flushed away by a dielectric is basically constant [22]. As the discharge energy increased,

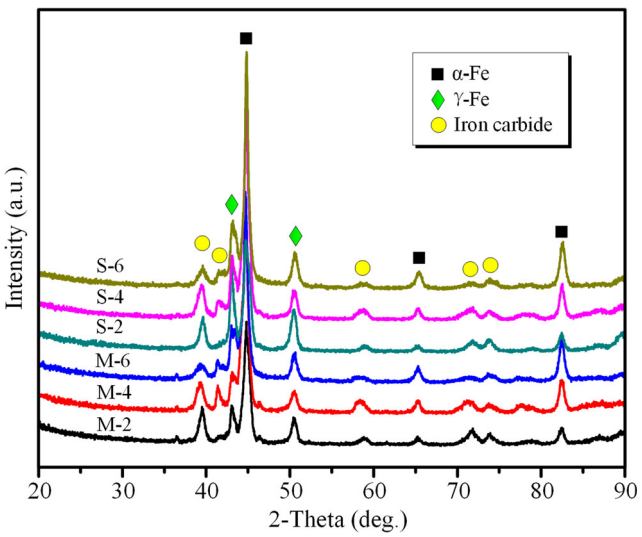

Fig. 15 XRD spectra of M-X and S-X (X = 2, 4, 6)

more heat energy acts on the surface of the sample during EDM, and thus increased the amount of molten material. Because the molten material cannot be further removed from the surface of the workpiece by the dielectric, it would accumulate on the surface. After discharge, the remaining molten materials are rapidly cooled and eventually formed a white layer on the workpiece surface. The thickness of the white layer depended on the amount of molten metal that was left on the surface during EDM. Therefore, the white layer thickness increased as the pulse-on time and current increased. In addition to pulse energy, electrode polarity was another important factor to influence the white layer thickness in this research. The evolution of white layer thickness in multi-step machining was similar to that in single-step machining. However, the average white layer thickness of M-X (X=1, 2, ···, 7) was higher than that of S-X. The difference in the thickness of the white layer between multi-step and single-step processed samples was less than 1.5 μm in our study. Świercz and Oniszczuk-Świercz have a similar finding in the research of surface layer properties of EDMed tool steel (In their study, the average thicknesses of the white layer of the EDMed tool steel with sequential and single-step processing were 5.5 μm and 5.24 μm, respectively.) [35]. The reasons for the difference were most likely owing to the material removal amount and material state at each step of processing. They thought that the differences between single-step and multi-step processing could be minimized by selecting the appropriate machining parameters.

3.5 Residual stress

Like other traditional machinings (e.g., turning and milling), the EDMed sample also has residual stress in the surface metamorphic layer. But differently, the existence of residual stress on the EDMed sample surface is usually presented as tensile stress. As we all know, the residual tensile stress on the components and parts would reduce their service life and even result in surface microcracks [36, 37]. Therefore, it is of great practical significance of the actual production to investigate the residual stress of the EDMed surface. Figure 18 displayed the residual stress of the STAVAX steel surface under different EDM conditions. It can be found from this figure that the residual stress on the surface of the EDMed sample was tensile stress, which was consistent with previous studies [2, 27–29]. From sample S-1 (M-1) to sample S-7 (M-7), the residual stress gradually decreased. The decreasing surface residual stress for single-step machining is mainly attributed to the reduction of discharge energy during EDM. When the discharge energy decreases, the heat transferred into the workpiece also decreases, thereby reducing the processing temperature. Consequently, the thermal stress and residual stress of EDMed surface also decreased. Compared with the single-step EDMed sample, the surface residual stress of the multi-step EDMed sample was slightly

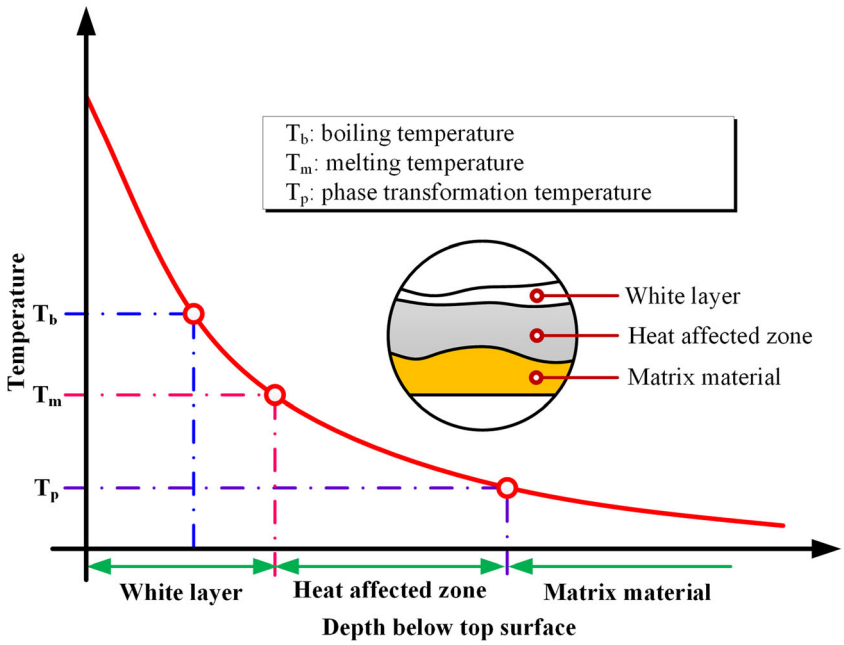

Fig. 16 Changes in temperature during the formation of the metamorphic layer

increased. The difference may be mainly ascribed to the influence of the material state after the previous processing.

4 Conclusions

This paper has presented the surface integrity evolution of STAVAX steel after EDM in the single-step and multi-step sequential machining. Meanwhile, the differences in surface integrity between single-step and multi-step EDM were also researched. The results showed that the evolution trend of surface integrity in these two machining conditions is similar. However, there were some differences between them in surface topography, roughness, white layer thickness, and residual stress. Some important findings in this study were summarized as follows.

(1) The surface roughness of the multi-step EDMed sample was higher than that of the single-step EDMed sample, and the difference became even larger in the finishing stage. In single EDM, surface roughness and morphology were mainly affected by electrical parameters. However, in multi-step EDM, the previous step during the machining process played an important role in the surface roughness and morphology of the sample obtained in the current step processing.

(2) There was no significant difference in the crystalline phase between single-step and multi-step processing. The crystalline phase of each EDMed sample was comprised of α-Fe, γ-Fe, and iron carbide.

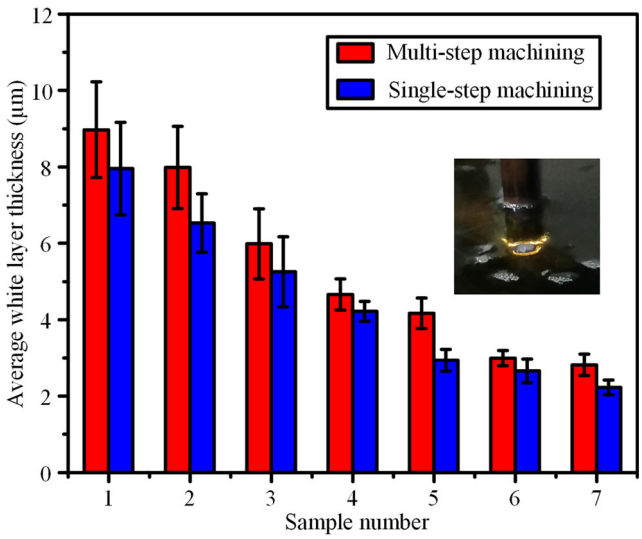

Fig. 17 The average white layer thickness of different samples

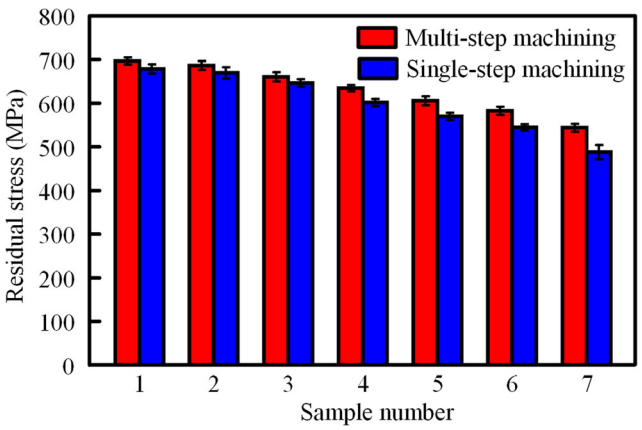

Fig. 18 Residual stress of different samples

(3) The average white layer thickness of the EDMed sample gradually decreased from roughing to finishing operations whether it was produced by single-step or multi-step machining. The white layer of the sample generated by multi-step EDM was thicker than that produced by single-step EDM. The difference in the average white layer thickness between multi-step and single-step processing was less than 1 μm in this study.
(4) Compared with single-step EDM, the surface residual stress of the multi-step EDMed sample slightly increased. With the decrease of discharge energy, the residual stress of the EDMed surface decreases gradually, but the variation trend of surface residual stress in single-step machining and multi-step machining is similar.
(5) When single-step machining is used to guide the actual multi-step machining, the surface integrity parameters obtained from single-step machining should be properly modified.

Acknowledgements The authors are thankful to Makino Asia China PTE. LTD. for the use of their machine tool.

Author contribution Guisen Wang: Conceptualization, methodology, experiment, validation, formal analysis, investigation, data curation, writing—original draft preparation, writing—review and editing; Fuzhu Han: Supervision, project administration, funding acquisition.

Funding The authors would like to acknowledge the National Key Foundation of China (61409230307) and the National Key R&D Program of China (2018YFB1105900).

Availability of data and materials All the data and materials of this work are available to the readers, according to the magazine policies.

Declarations

Ethics approval and consent to participate The authors claim that there are no ethical issues involved in this research. All the authors consent to participate in this research and contribute to the research.

Consent for publication All the authors consent to publish the research. There are no potential copyright/plagiarism issues involved in this research.

Competing interests The authors declare no competing interests.

References

1. Abbas NM, Solomon DG, Bahari MF (2007) A review on current research trends in electrical discharge machining (EDM). Int J Mach Tool Manu 47(7-8):1214–1228. https://doi.org/10.1016/j.ijmachtools.2006.08.026
2. Merdan MAER, Arnell RD (1991) The surface integrity of a die steel after electro-discharge machining: 2 residual stress distribution. Surf Eng 7(2):154–158. https://doi.org/10.1179/sur.1991.7.2.154
3. Sidhom H, Ghanem F, Amadou T, Gonzalez G, Braham C (2013) Effect of electro-discharge machining (EDM) on the AISI316L SS white layer microstructure and corrosion resistance. Int J Adv Manuf Technol 65(1-4):141–153. https://doi.org/10.1007/s00170-012-4156-6
4. Gostimirovic M, Kovac P, Sekulic M, Skoric B (2012) Influence of discharge energy on machining characteristics in EDM. J Mech Sci Technol 26(1):173–179. https://doi.org/10.1007/s12206-011-0922-x
5. Das S, Klotz M, Klocke F (2003) EDM simulation: finite element-based calculation of deformation, microstructure and residual stresses. J Mater Process Technol 142(2):434–451. https://doi.org/10.1016/s0924-0136(03)00624-1
6. Ekmekci B, Elkoca O, Erden A (2005) A comparative study on the surface integrity of plastic mold steel due to electric discharge machining. Metall Mater Trans B Process Metall Mater Process Sci 36(1):117–124. https://doi.org/10.1007/s11663-005-0011-6
7. Dewangan S, Gangopadhyay S, Biswas CK (2015) Study of surface integrity and dimensional accuracy in EDM using Fuzzy TOPSIS and sensitivity analysis. Measurement 63:364–376. https://doi.org/10.1016/j.measurement.2014.11.025
8. Lee HT, Hsu FC, Tai TY (2004) Study of surface integrity using the small area EDM process with a copper–tungsten electrode. Mater Sci Eng A 364(1-2):346–356. https://doi.org/10.1016/j.msea.2003.08.046
9. Zeilmann RP, Bordin FM, Vacaro T (2015) Surface integrity of electro-discharge machined cavities for different depths and radii. J Braz Soc Mech Sci 37(1):93–104. https://doi.org/10.1007/s40430-014-0159-6
10. Guo YB, Li W, Jawahir IS (2009) Surface integrity characterization and prediction in machining of hardened and difficult-to-machine alloys: a state-of-art research review and analysis. Mach Sci Technol 13(4):437–470. https://doi.org/10.1080/10910340903454922
11. Das AK, Kumar P, Sethi A, Singh PK, Hussain M (2016) Influence of process parameters on the surface integrity of micro-holes of SS304 obtained by micro-EDM. J Braz Soc Mech Sci 38(7):2029–2037. https://doi.org/10.1007/s40430-016-0488-8
12. Pradhan MK (2013) Estimating the effect of process parameters on surface integrity of EDMed AISI D2 tool steel by response surface methodology coupled with grey relational analysis. Int J Adv Manuf Technol 67(9-12):2051–2062. https://doi.org/10.1007/s00170-012-4630-1
13. Kiyak M, Aldemir BE, Altan E (2015) Effects of discharge energy density on wear rate and surface roughness in EDM. Int J Adv Manuf Technol 79(1-4):513–518. https://doi.org/10.1007/s00170-015-6840-9
14. Kiyak M, Çakır O (2007) Examination of machining parameters on surface roughness in EDM of tool steel. J Mater Process Technol 191(1-3):141–144. https://doi.org/10.1016/j.jmatprotec.2007.03.008
15. Lee HT, Tai TY (2003) Relationship between EDM parameters and surface crack formation. J Mater Process Technol 142(3):676–683. https://doi.org/10.1016/S0924-0136(03)00688-5
16. Rizvi SAH, Agarwal S (2016) An investigation on surface integrity in EDM process with a copper tungsten electrode. Procedia CIRP 42:612–617. https://doi.org/10.1016/j.procir.2016.02.254
17. Amorim FL, Weingaertner WL (2005) The influence of generator actuation mode and process parameters on the performance of finish EDM of a tool steel. J Mater Process Technol 166(3):411–416. https://doi.org/10.1016/j.jmatprotec.2004.08.026
18. Chakraborty S, Dey V, Ghosh SK (2015) A review on the use of dielectric fluids and their effects in electrical discharge machining characteristics. Precis Eng 40:1–6. https://doi.org/10.1016/j.precisioneng.2014.11.003
19. Kumar V, Kumar A, Kumar S, Singh NK (2018) Comparative study of powder mixed EDM and conventional EDM using

response surface methodology. Materials Today: Proceedings 5(9): 18089–18094. https://doi.org/10.1016/j.matpr.2018.06.143
20. Lim LC, Lee LC, Wong YS, L H H (1991) Solidification microstructure of electro-discharge machined surfaces of tool steels. Mater Sci Technol 7(3):239–248. https://doi.org/10.1179/026708391790183411
21. Ekmekci B (2007) Residual stresses and white layer in electric discharge machining (EDM). Appl Surf Sci 253(23):9234–9240. https://doi.org/10.1016/j.apsusc.2007.05.078
22. Bozkurt B, Gadalla AM, Eubank PT (1996) Simulation of erosions in a single discharge EDM process. Mater Manuf Process 11(4): 555–563. https://doi.org/10.1080/10426919608947508
23. Pecas P, Henriques E (2008) Electrical discharge machining using simple and powder-mixed dielectric: the effect of the electrode area in the surface roughness and topography. J Mater Process Technol 200(1-3):250–258. https://doi.org/10.1016/j.jmatprotec.2007.09.051
24. Tzeng Y, Chen F (2005) Investigation into some surface characteristics of electrical discharge machined SKD-11 using powder-suspension dielectric oil. J Mater Process Technol 170(1-2):385–391. https://doi.org/10.1016/j.jmatprotec.2005.06.006
25. Tang J, Yang X (2018) Simulation investigation of thermal phase transformation and residual stress in single pulse EDM of Ti–6Al–4V. J Phys D Appl Phys 51(13):135308. https://doi.org/10.1088/1361-6463/aab1a8
26. Liu JF, Guo YB (2016) Residual stress modeling in electric discharge machining (EDM) by incorporating massive random discharges. Procedia CIRP 45:299–302. https://doi.org/10.1016/j.procir.2016.02.060
27. Mehmood S, Sultan A, Anjum N A, Anwar W, Butt Z (2017) Determination of residual stress distribution in high strength aluminum alloy after EDM. Adv Sci Technol Res J 11(1):29–35. https://doi.org/10.12913/22998624/68729
28. Guu YH, Hocheng H, Chou CY, Deng CS (2003) Effect of electrical discharge machining on surface characteristics and machining damage of AISI D2 tool steel. Mater Sci Eng A 358(1-2):37–43. https://doi.org/10.1016/s0921-5093(03)00272-7
29. Li XS, Cai AH, Zeng JJ (2012) Effect of EDM conditions on surface residual stress of Cr12MoV steel. Mater Sci Forum 697:171–175. https://doi.org/10.4028/www.scientific.net/MSF.697-698.171
30. Tanaka K (2018) X-ray measurement of triaxial residual stress on machined surfaces by the cosα method using a two-dimensional detector. J Appl Crystallogr 51:1329–1338. https://doi.org/10.1107/S1600576718011056
31. Wang JS, Hsieh CC, Lai HH, Kuo CW, Wu PT, Wu W (2015) The relationships between residual stress relaxation and texture development in AZ31 Mg alloys via the vibratory stress relief technique. Mater Charact 99:248–253. https://doi.org/10.1016/j.matchar.2014.09.019
32. Ekmekci B (2009) White layer composition, heat treatment, and crack formation in electric discharge machining process. Metall Mater Trans B Process Metall Mater Process Sci 40(1):70–81. https://doi.org/10.1007/s11663-008-9220-0
33. Jahan MP, Wong YS, Rahman M (2009) A study on the fine-finish die-sinking micro-EDM of tungsten carbide using different electrode materials. J Mater Process Technol 209(8):3956–3967. https://doi.org/10.1016/j.jmatprotec.2008.09.015
34. Wu KL, Yan BH, Huang FY, Chen SC (2005) Improvement of surface finish on SKD steel using electro-discharge machining with aluminum and surfactant added dielectric. Int J Mach Tool Manu 45:1195–1201. https://doi.org/10.1016/j.ijmachtools.2004.12.005
35. Świercz R, Oniszczuk-Świercz D (2017) Experimental investigation of surface layer properties of high thermal conductivity tool steel after electrical discharge machining. Metals 7(12):1–16. https://doi.org/10.3390/met7120550
36. Mower TM (2014) Degradation of titanium 6Al–4V fatigue strength due to electrical discharge machining. Int J Fatigue 64: 84–96. https://doi.org/10.1016/j.ijfatigue.2014.02.018
37. Tai TY, Lu SJ (2009) Improving the fatigue life of electro-discharge-machined SDK11 tool steel via the suppression of surface cracks. Int J Fatigue 31(3):433–438. https://doi.org/10.1016/j.ijfatigue.2008.07.013